(3) Absorption of Light

In explaining the colors of coordination compounds, we are dealing with the phenomenon of complementary colors: if a compound absorbs light of one color, we see the complemnt of that color. For example, when white light (containing a broad spectrum of all visible wavelengths) passes through a substance that absorbs red light, the color observed is green. Green is the complement of red, so green predominates visually when red light is subtracted from white. Complementary colors can conveniently be remembered as the color pairs on opposite sides of the color wheel shown below.

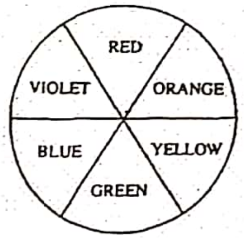

An example from coordination chemistry is the deep blue color of aqueous solutions of copper (II) compounds, containing the ion $[Cu(H_2O)_6]^{2+}$. The blue color is a consequence of the absorption of light between approximately 600 and 1000 nm (maximum near 800 nm;), in the yellow to infrared region of the spectrum. The color observed, blue, is the average complementary color of the light absorbed.

It is not always possible to make a simple prediction of color directly from the absorption spectrum, in large part because many coordination compounds contain two or more absorption bands of different energies and intensities. The net color observed is the color predominating after the various absorption are removed from white light.

BEER-LAMBERT ABSORPTION LAW

If light of intensity I_0 at a given wavelength passes through a solution containing a species that absorbs light, the light emerges with intensity I, which may be measured by a suitable detector.

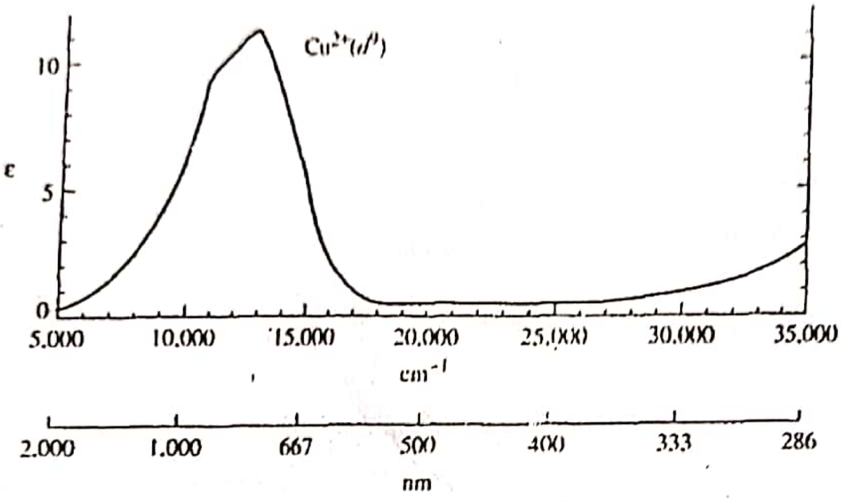

Visible Light and Complementary Colors

Wavelength Range (nm)	Wave numbers (cm^{-1})	Color	Complementary color
< 400	> 25,000	Ultraviolet	
400–450	22,000–25,000	Violet	Yellow
450–490	20,000–22,000	Blue	Orange
490–550	18,000–20,000	Green	Red
550–580	17,000–18,000	Yellow	Violet
580–650	15,000–17,000	Orange	Blue
650–700	14,000–15,000	Red	Green
> 700	< 14,000	Infrared	

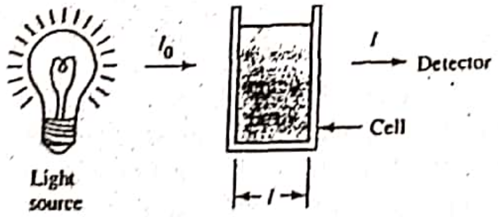

The Beer-Lambert law may be used to describe the absorption of light (ignoring scattering and reflection of light from cell surfaces) at a given wavelength by an absorbing species in solution:

$$\log\frac{I_0}{I} = A = \varepsilon l c$$

where A = absorbance
ε = molar absorptivity (L mol^{-1} cm^{-1}) (also known as molar extinction coefficient)
l = path length through solution (cm)
c = concentration of absorbing species (mol L^{-1})

Absorbance is a dimensionless quantity. An absorbance of 1.0 corresponds to 90% absorption at a given wavelength, an absorbance of 2.0 corresponds to 99% absorption and so on.

Spectrophotometers commonly obtain spectrum as plots of absorbance versus wavelength. The molar absorptivity is a characteristic of the species that is absorbing the light and is highly dependent on wavelength. A plot of molar absorptivity versus wavelength gives a spectrum characteristic of the molecule or ion in question, figure. As we will see, this spectrum is a consequence of transitions between states of different energies and can provide valuable information about those states and in turn, about the structure and bonding of the molecule or ion.

Although the quantity most commonly used to describe absorbed light is the wavelength, energy and frequency are also used. In addition , the wavenumber the number of waves per centimeter, a quantity propotional to the energy, is frequently used. For reference, the relations between these quantities are given by the equations.

$$\Delta E = h\nu = \frac{hc}{\lambda} = hc\left(\frac{1}{\lambda}\right) = hc\bar{\nu}$$

$$\therefore \quad \Delta E \propto \frac{1}{\lambda} \propto \bar{\nu}$$

where ΔE = energy

h = Planck's constant = 6.626×10^{-34} J s

c = speed of light = 2.998×10^{8} ms^{-1}

ν = frequency (s^{-1})

λ = wavelength (often reported in nm)

$\frac{1}{\lambda} = \bar{\nu}$ = wavenumber (cm^{-1})

Selection rule

$$\left.\begin{array}{l}\Delta l = \pm 1\\ \Delta s = 0\end{array}\right\}\ \text{Net 2015 Dec}$$

(4) Laporte 'Orbital' Selection Rule

Transitions which involve a change in the subsidiary quantum number ($\Delta l = \pm 1$ are 'Laporte allowed') and therefore have a high absorbance. If $\Delta\, l = 0$ i.e., there is no change in subsidiary quantum number, then transions are said to be forbidden. Laporte selection rule may also be given as follows:

Transitions between g (gerade) and u (ungerade) orbitals are permitted and the transition between g orbitals or u orbitals are not permitted.

$$g \longleftrightarrow u \qquad g \not\longleftrightarrow g \qquad u \not\longleftrightarrow u$$

Thus for Ca, $s^2 \rightarrow s^1p^1, l$ changes by + 1 and the molar absorption coefficient ε is 5000–10,000 litres per mol per centimetre. In contrast *d-d* transition are 'Laporte forbidden', since the change in l = 0, but spectra of much lower absorbance are absorbed ($\varepsilon = 5 - 10\ l\ \text{mol}^{-1}\ \text{cm}^{-1}$) because of slight relaxation in the Laporte rule. When the transition metal ion forms a complex it is surrounded by ligands, and some mixing of *d* and *p* orbitals may occur, in which case transitions are no longer pure *d-d* in nature. Mixing of this kind occurs in complexes which do not possess a centre of symmetry, for example tetrahedral complexes, or asymmetrically substituted octahedral complexes. Thus $[MnBr_4]^{2-}$ which is tetrahedral and $[Co(NH_3)_5Cl]^{2+}$ which is octahedral but non-centrosymmetric are both coloured. Mixing of *p* and *d* orbitals does not occur in octahedral complexes which have a centre of symmetry such as $[Co(NH_3)_6]^{3+}$ or $[Cu(H_2O)_6]^{2+}$. However, in these cases the metal-ligands bonds vibrate so that the ligands spend an appreciable amount of time out of their centro-symmetric equilibrium position. Thus a very small amount of mixing occurs and low-intensity spectra are observed. Thus Laporte allowed transitions are very intense, whilst Laporte forbidden transitions vary from weak intensity if the complex in non-centrosymeetric to very weak if it is centrosymmetric. Since *p-d* is more pronounced in tetrahedral complexes (non-centro symmetric) than octahedral complexes (centro symmetric). Thus tetrahedral complexes give more intense colour than octahedral complexes.

Spin Selection Rule

During transitions between energy levels, an electron does not change its spin, that is $\Delta S = 0$ i.e., any transition for which $\Delta S = 0$ (no change in spin state) is allowed. if $\Delta S \neq 0$ (change in spin state) transition is forbidden. In other words, for allowed transitions spin multiplicity does not change. e.g.,

$${}^3T_{2g} \longrightarrow {}^3T_{2g}$$

$${}^3T_{1g} \longrightarrow {}^3A_{2g}$$

$${}^3T_{1g} \longrightarrow {}^3T_{1g(P)}$$

There are fewer exceptions than for the Laporte selection rule. Thus in the case of Mn^{2+} in a weak octahedral field such as $[Mn(H_2O)_6]^{2+}$ the *d-d* transitions are spin forbidden because each of the *d* orbitals is singly occupied. Many Mn^{2+} compounds are off white or pale flesh coloured, but the intensity is only about one hundredth of that for a spin allowed transition. Since the spin forbidden transitions are very weak, analysis of the spectra of transition metal complexes can be greatly simplified by ignoring all spin forbidden transitions and considering only those excited states which have the same multiplicity as the ground state. Thus for a d^2 configuration the only terms which need be considered are the ground state ^3F and the excited state ^3P.

Ti^{3+} in weak octahedral field (spin allowed), if electron in t_{2g} level is excited to e_g level then spin state will not change. Thus this transition is spin allowed.

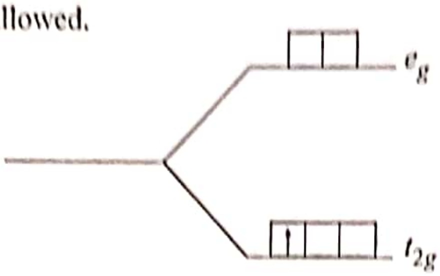

Mn^{2+} in weak octahedral field (spin forbidden transition), if one of the electrons in t_{2g} level is excited to e_g state then spin state is changed (from clockwise to anticlockwise) thus this electronic transition is spin forbidden.

Tetrahedral → p-d mixing
Octahedral → vibronic coupling

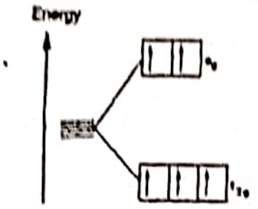

Molar absorption coefficient for different types of transition are given in the following table:

Laporte (orbital)	Spin	Type of Spectra	ε (L mol^{-1} cm^{-1})	Example
Allowed	Allowed	Charge transfer	10000	$[TiCl_6]^{2-}$
Partly alllowed, some *p-d* mixing	Allowed	*d-d*	500	$[CoBr_4]^{2-}\cdot[CoCl_4]^{2-}$
Forbidden	Allowed	*d-d*	8–10	$[Ti(H_2O)_6]^{3+}\cdot[V(H_2O)_6]^{3+}$
Partly allowed, some *p-d* mixing	Forbidden	*d-d*	4	$[MnBr_4]^{2-}$
Forbidden	Forbidden	*d-d*	0.02	$[Mn(H_2O)_6]^{2+}$

(5) Splitting of Electronic Energy Levels and Spectroscopic States

An *s* orbital is spherically symmetrical and is unaffected by an octahedral (or any other) field, *p* orbitals are directional, and *p* orbitals are affected by an octahedral field. However, since a set of three *p* orbitals are all affected equally, their energy levels remain equal, and no splitting occurs. A set of *d* orbtials is split by an octahedral field into two level t_{2g} and e_g The difference in energy between these may be written as Δ_0 or $10D_q$. The t_{2g} level is triply degenerate and is $-4D_q$ below the barycentre and the e_g level is doubly degenerate and is $6D_q$ above the barycentre. For a d^1 configuration, the ground state is a 2_D state, and the t_{2g} and e_g electronic energy levels correspond with the T_{2g} and E_g spectroscopic states. A set of *f* orbitals is split by an octahedral field into three levels. For an f^1 arrangement the ground state is a ^3F state and is split into a triply degenerate T_{1g} state which is $6D_q$ below the barycentre, a triply degenerate T_{2g} level which is $2D_q$ above the barycentre and a single A_{2g} state which is $12D_q$ above the barycentre.

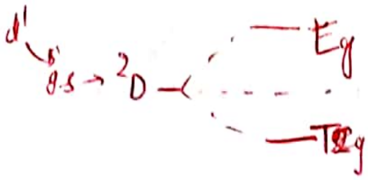

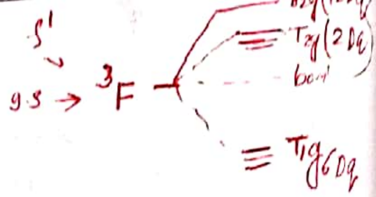

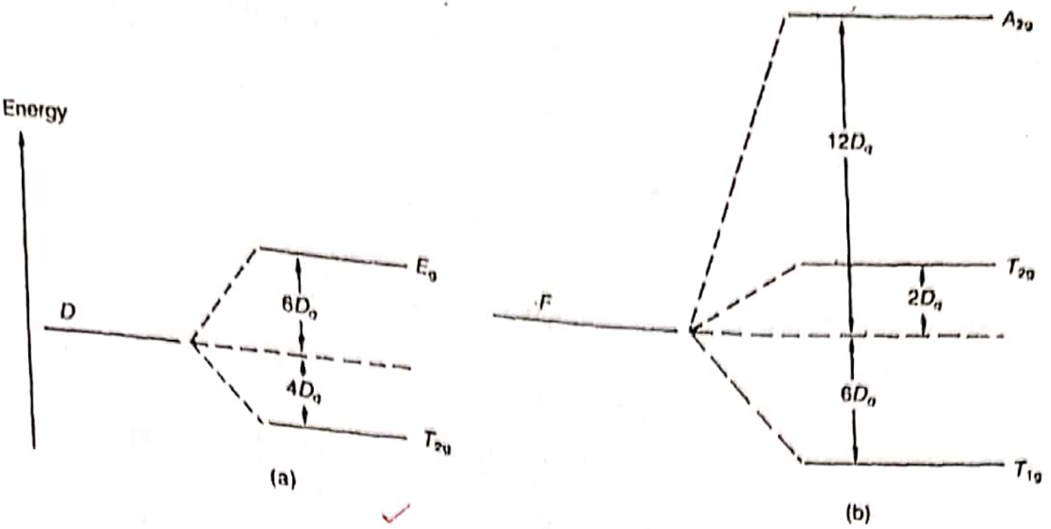

A_2
T_2
T

In the one electron cases s^1, p^1, d^1 and f^1 there is a direct correspondence between the splitting of electronic energy levels which occurs in a crystal field and the splitting of spectroscopic states. Thus in an octahedral field the S and P states are not split. D states are split into two states and F states are split into three states.

Table : Transforming spectroscopic terms into Mulliken symbols

Spectroscopic term	**Mulliken Symbols**	
	Octahedral field	**Tetrahedral field**
S	A_{1g}	A_1
P	T_{1g}	T_1
D	$E_g + T_{2g}$	$E + T_2$
F	$A_{2g} + T_{1g} + T_{2g}$	$A_2 + T_1 + T_2$
$P+D = G$ G	$A_{1g} + E_g + T_{1g} + T_{2g}$	$A_1 + E + T_1 + T_2$

(6) Table

Ground and excited terms having the same spin multiplicities for weak field octahedral (oct) and tetrahedral (tet) complexes

Configuration	**Ground term**	**Excited terms with the same spin multiplicity as the ground term**
d^1 oct, d^9 tet d^n, d^{10-n}	${}^2T_{2(g)}$	${}^2E_{2(g)}$
d^2 oct, d^8 tet	${}^3T_{1(g)}F$	${}^3T_{2(g)}, {}^3A_{2(g)}, {}^3T_{1(g)},(P)$
d^3 oct, d^7 tet	${}^4A_{2(g)}$	${}^4T_{2(g)}, {}^4T_{1(g)}(F), {}^4T_{1(g)}(P)$
d^4 oct, d^6 tet	${}^5E_{2(g)}$	${}^2T_{2(g)}$
d^5 oct, d^5 tet	${}^6A_{1(g)}$	None
d^6 oct, d^4 tet	${}^5T_{2(g)}$	${}^5E_{2(g)}$
d^7 oct, d^3 tet	${}^4T_{1(g)}(F)$	${}^4T_{2(g)}, {}^4A_{2(g)}, {}^4T_{1(g)}(P)$
d^8 oct, d^2 tet	${}^3A_{2(g)}$	${}^3T_{2(g)}, {}^3A_{1(g)}(F), {}^3T_{1(g)}(P)$
d^9 oct, d^1 tet	${}^2E_{2(g)}$	${}^2T_{2(g)}$

d^n octahedral $= d^{10-n}$ td.

Configuration **Correlation of Spectroscopic Ground Term**

1. d^1

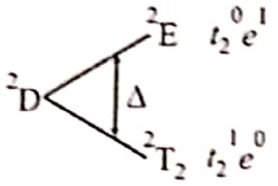

2. d^2 ^3P .... $^3T_1$ t_2^1 e^1

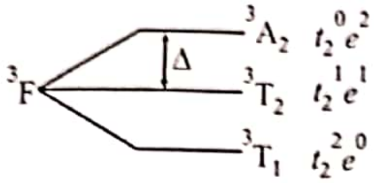

3. d^3 ^4P .... $^4T_1$ t_2^1 e^1

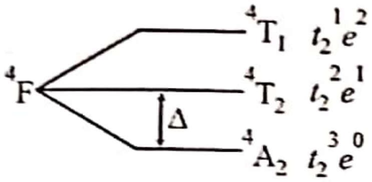

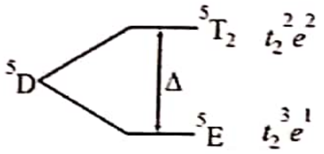

4. d^4

5. d^5 ^6S .... $^6A_1$ t_2^3 e^2

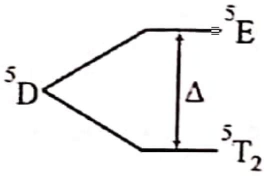

6. d^6

7. d^7 ^4P $^4T_1$

8. d^8 and d^9 inverse of d^2

(7) Spectra of d^1 and d^9 Ions

In a free gaseous metal ion the *d* orbitals are degenerate, and hence there will be no spectra from *d-d* transitions. When a complex is formed, the electrostatic field from the legands splits the *d* orbitals into two groups t_{2g} and e_g. The simplest example of a d^1 complex is Ti(III) in octahedral complexes such as $[TiCl_6]^{3-}$ or $[Ti(H_2O)_6]^{3+}$. The splitting of the *d* orbitals is shown in the following figure (a). In the ground state the single electron occupies the lower t_{2g} level, and only one transition is possible to the e_g level. Consequently the absorption spectrum of $[Ti(H_2O)_6]^{3+}$ which is shown in figure (b) shows only one band with a peak at 20300 cm^{-1}. The magnitude of the splitting Δ_0 depends on the nature of the ligands, and affects the energy of the transition, and hence the frequency of maximum absorption in the spectrum. Thus the peak occurs at 13000 cm^{-1} in $[TiCl_6]^{3-}$, 18900 cm^{-1} in $[TiF_6]^{3-}$, 20300 cm^{-1} in $[Ti(H_2O)_6]^{3+}$ and 22300 cm^{-1} in $[Ti(CN)_6]^{3-}$. The amount of splitting caused by various ligands is related to their position in the spectrochemical series. The symbol ^2D at the left is the ground state term for a free ion with a d^1 configuration. Under the influence of a ligand field this splits into two states which are described by the

Mulliken symbols ^2E_g and $2T_{2g}$. The lower $2T_{2g}$ state corresponds to the single *d* electron occupying one of the t_{2g} orbitals, and the ^2E_g state corresponds to the electron occupying one of the e_g orbitals. The two states are separated more widely as the strength of the ligand field increases.

2tg

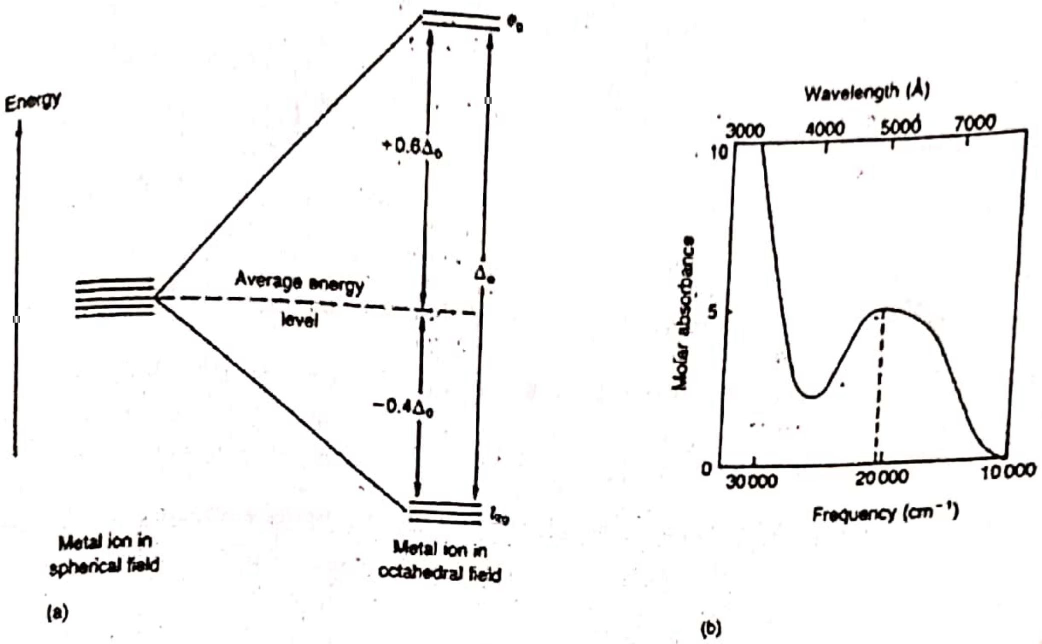

Fig. (a) Diagram of energy levels in octahedral field. (b) Ultraviolet and visible absorption spectrum of $[Ti(H_2O)_6]^{3+}$

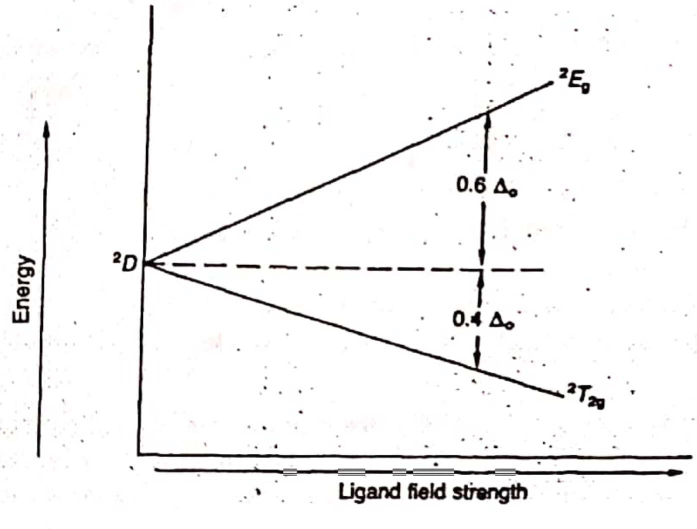

d^n - octahedral = d^{10-n} + d
↳ inverse of d^{10-n} octahedral
⇓
d^{n+5} octahedral

Fig. Splitting of energy levels for d^1 configuration in octahedral field.

Octahedral complexes of ions with a d^9 configuration such as $[Cu(H_2O)_6]^{2+}$ can be described in a similar way to the Ti^{3+} octahedral complexes with a d^1 arrangement. In the d^1 case there is a single electron in the lower t_{2g} level whilst in the d^9 case there is a single hole in the upper e_g level. Thus the transition in the d^1 case is promoting an electron from the t_{2g} level to the e_g level, whilst in the d^9 case it is simpler to consider the promotion of an electron as the transfer of a 'hole' from e_g to t_{2g}. The energy diagram for d^9 is therefore is the inverse of that for a d^1 configuration.

The effect of a tetrahedral ligand field is now considered, the degenerate *d* orbitals split into two e_g orbitals of lower energy and three t_{2g} orbitals of higher energy. The energy level diagram for d^1 complexes in a tetrahedral field is the inverse of that in an octahedral field, and is similar to the d^9 octahedral case, except that the amount of splitting in a tetrahedral field is only about $\frac{4}{9}$ of that in an octahedral field.

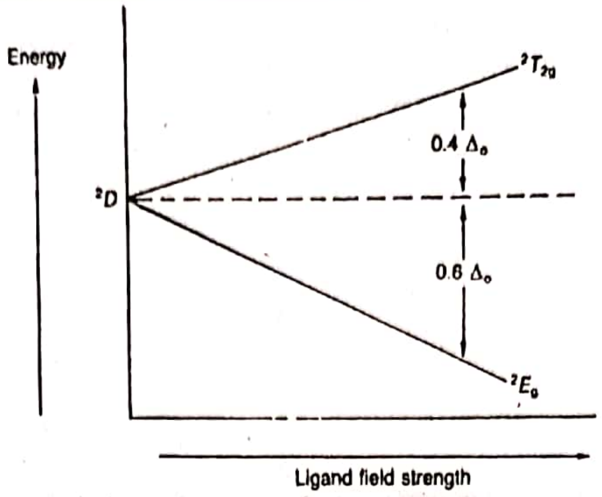

Figure. Splitting of energy levels for d^9 configuration in octahedral field

In a similar way the d^6 high-spin octahedral arrangement is related to the d^1 octahedral case. Since transitions which involve reversal of the electron spin are 'forbidden', and hence give extremely weak bands, the only 'permitted' transition is the paired electron in the t_{2g} level, which has the opposite spin to all the other electrons, to the e_g level. The energy level diagram for d^6 high-spin octahedral complexes is the same as the d^1 case.

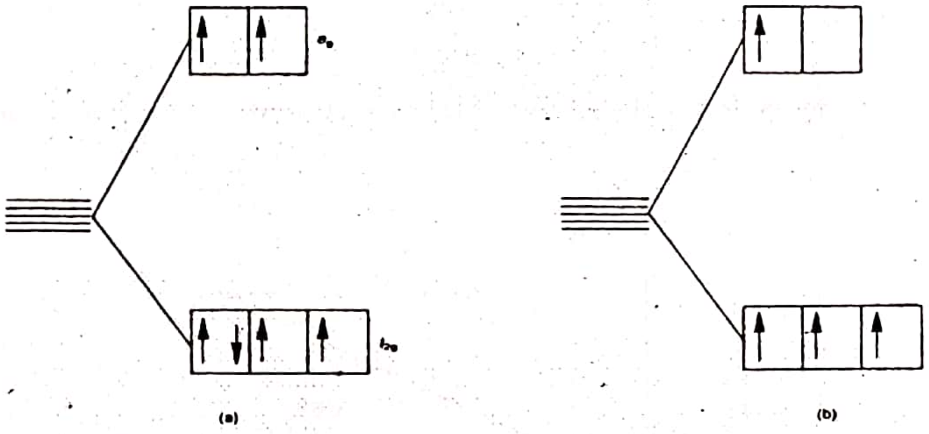

Fig. (a) d^6 and (b) d^4 high-spin octahedral arrangements

$d^6 Td = d^1 Td = d^9$ octahe

$d^1 td = d^9 Td = d^2$ octahed

By similar reasoning, octahedral complexes containing d^4 ions in a high-spin arrangement may be considered as having one 'hole' in the upper e_g level and thus they are analogous to the d^9 octahedral case.

$d^n = d^{5+n}$

In addition, d^6 tetrahedral complexes have only one electron which can be promoted without changing the spin, and have a diagram like that for d^1 tetrahedral, which is qualitatively similar to that for the d^9 octahedral case. Finally, d^4 and d^9 tetrahedral complexes with one 'hole' are qualitatively like the d^1 octahedral example with one electron.

Orgel diagram

Above figures can be combined into a single diagram calld an orgel diagram, which describes in a qualitative way the effect of electron configurations with one electron, One electron more than a half filled level, one electron less than a full shell, and one electron less than a half filled shell.

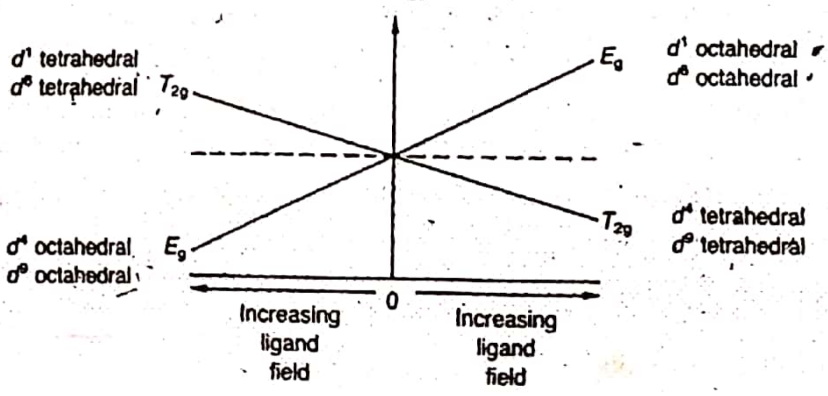

$d^n oct = d^{n+5}$ octa

$d^n td = d^{n+5} td$

$d^6 td = d^{10-6} = d^4$ octa

d^1 ted

Fig. Orgel combined energy level diagram for d^1 (Note that g subscripts are dropped in tetrahedral cases)

(8) Spectra of d^2 and d^8 ions

The ground state for a d^2 electronic arrangement has two electrons in different orbitals. In an octahedral field the d orbitals are split into three t_{2g} orbitals of lower energy and two e_g orbitals of higher energy, and the electrons will occupy two of the t_{2g} orbitals. When an electron is promoted $t_{2g}^2 \rightarrow (e_g)^1(t_{2g})^1$ there are two possibilities. It requires less energy to promote an electron from the d_{xy} or d_{yz} orbitals to the d_{z^2} orbital than it does to promote the electron to the $d_{x^2-y^2}$ orbital. This difference in energy arises because the former transition gives $(d_{xy})^1(d_{z^2})^1$ arrangement where the electrons are spread around all three direction x, y and z which reduces electron-electron repulsion compared with the $(d_{xy})^1(d_{x^2-y^2})^1$ arrangement where the electrons are confined to the xy plane. If both electrons are promoted another high energy state will be formed. Thus from a consideration of the electrons we would expect four energy levels.

The terms arising for a d^2 configuration are the ground state ^3F and the excited states ^3P, ^1G, ^1D and ^1S. The ^3P ground state contains two electrons with parallel spins, but the ^1G, ^1D and ^1S states contain electrons with opposite spins. Thus transitions from the ground state to these three states are spin forbidden, will be very weak, and can be ignored. The two remaining state ^3F and ^3P can have spin permitted transitons. It will be remembered that p orbitals are not split by an octahedral field, but that f orbitals are split into three levels. Similarly in an octahedral field P states are not split (but are transformed into a T_{1g} state, and F states split into $A_{2g} + T_{1g} + T_{2g}$. The energy level diagram for these is shown in figure. Three transitions are possible from the ground state $^3T_{1g}(F)$ to $^3T_{2g}$, $^3T_{1g}(P)$ and $^3A_{2g}$ respectively, and hence three peaks should appear in the spectrum. (Ground state terms for $d^1 - d^{10}$ configurations)

Configuration	Example	Ground term	m_l					M_L	S
			2	1	0	−1	−2		
d^1	Ti^{3+}	^2D	↑					2	½
d^2	V^{3+}	^3F	↑	↑				3	1
d^3	Cr^{3+}	^4F	↑	↑	↑			3	1½
d^4	Cr^{2+}	^5D	↑	↑	↑	↑		2	2
d^5	Mn^{2+}	^6S	↑	↑	↑	↑	↑	0	2½
d^6	Fe^{2+}	^5D	↑↓	↑	↑	↑	↑	2	2
d^7	Co^{2+}	^4F	↑↓	↑↓	↑	↑	↑	3	1½
d^8	Ni^{2+}	^3F	↑↓	↑↓	↑↓	↑	↑	3	1
d^9	Cu^{2+}	^2D	↑↓	↑↓	↑↓	↑↓	↑	2	½

The spectrum of d^2 complex ion $[V(H_2O)_6]^{3+}$ is shown in figure. Only two peaks occur in this spectrum because the ligand field strength of water results in transitons occurring close to the cross-over point between the $^3T_{1g}(P)$ and $^3A_{2g}$ levels, and hence these two transitions are not resolved into two separate peaks. A V^{3+} ion complexed with a different ligand would show three peaks.

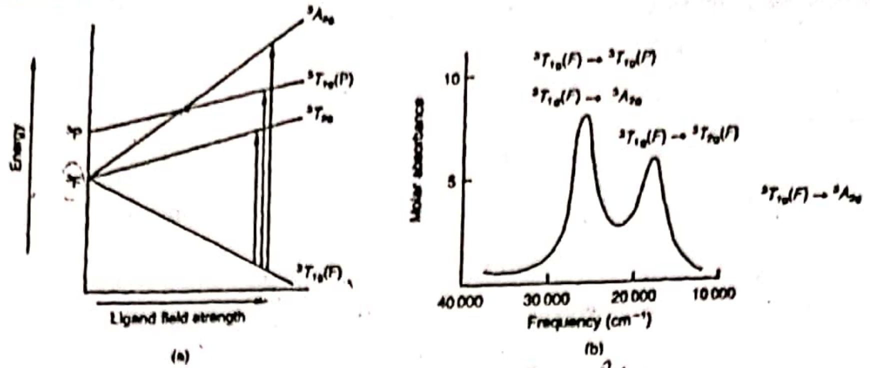

Fig. Orgel diagram and spectrum for a d^2 ion.

Complexes of metals such as Ni^{2+} with a d^8 configuration in an octahedral field can be treated in a similar way. There are two 'holes' in the e_g level, and hence promoting an electron is equivalent to transferring a 'hole' from e_g to t_{2g}. This is the inverse of the d^2 case. The ^3P state is not split, and is not inverted, but the ^3F state is split into three states and is inverted. Thus the ground state term for Ni^{2+} is $^3A_{2g}$. Note that in both the d^2 case and the d^8 case the ^3F state is the lowest in energy.

Three spin allowed transitions are observed in the spectra of $[Ni(H_2O)_6]^{2+}$, $[Ni(NH_3)_6]^{2+}$ and $[Ni(ethylenediamine)_3]^{2+}$.

Using the same arguments as applied to the d^1 case, the d^2 octahedral energy diagram is similar to the high-spin d^7 octahedral, and d^3 and d^8 tetrahedral cases. The inverse diagram applies to the d^3 and d^8 octahedral as well as d^2 and d^7 tetrahedral complexes. As before, the g subscript is omitted in tetrahedral complexes.

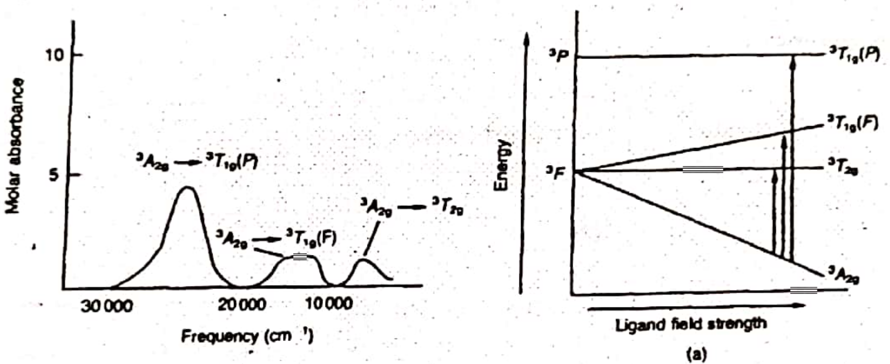

Fig. Orgel diagram and spectrum for a d^8 ion.

In a similar way Cr(III) has a d^3 configuration, and for octahedral complexes the inverted diagram at the left hand side of figure applies. This is similar to the d^2 diagram except that the energies of the three states derived from the ^3F state are inverted in order. The spectra of chromium octahedral complexes would be expected to show three absorption bands from the ground state $3A_{2g}$ to $^3T_{2g}$, $^3T_{1g}(F)$ and $^3T_{1g}(P)$ respectively.

Chromium (III) complexes show at least two well defined absorption peaks in the visible region. In some cases the third band can be seen, though it is often hidden by a very intense charge transfer band.

The combined Orgel energy level diagram for two-electron and two-'hole' configurations is shown in following figure. Note that there are two T_{1g} states, one from the P state and the other from the F state. The two T_{1g} states are slightly curved lines, because they have the same symmetry, and they interact with one another. This interelectronic repulsion lowers the energy of the lower state and increases the energy of the higher state. The effect is much more marked on the left of the diagram because the two levels are close in energy. If the lines had been straight, they would cross each other, implying at the cross over point that two electrons in one atom may have the same symmetry and the same energy. This would be impossible, and is prohibited by the non-crossing rule, which says that states of the same symmetry cannot cross each other. The mixing or interelectronic repulsion which causes the bending of the lines is expressed by the Racah parameters B and C.

Racah Parameters

1. Coulombic repulsion exists among electrons in molecular orbitals of the complexes therefore different terms of a configuration have different energies. The repulsion energy of each term of a configuration is expressed as sums of three quantities. The three different sums of three quantities. The three different sums of integrals

The pale pink colour of many octahedral complexes of Co(II) are of interest. The spectrum of $[Co(H_2O)_6]^{2+}$ is shown in figure.

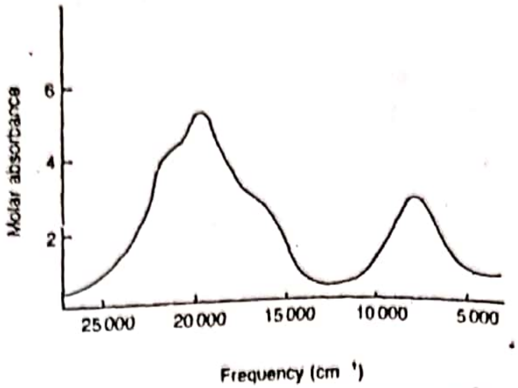

Fig. Electronic spectrum of $[Co(H2O)6]^{2+}$

d^7

The spectrum of $[Co(H_2O)_6]^{2+}$ is less easy to interpret. It shows a weak but well resolved absorption band at about 8000 cm^{-1}, and a multiple absorption band comprising three overlapping peaks at about 20000 cm^{-1}. The lowest energy band ν_1 at 8000 cm^{-1} is assigned to the ${}^4T_{1g} \rightarrow {}^4T_{2g}$ transition. The multiple band has three peaks at about 16000, 19400 and 21600 cm^{-1}. Two of these are the ${}^4T_{1g} \rightarrow {}^4A_{2g}$ and ${}^4T_{1g} \rightarrow {}^4T_{1g}(P)$ transitions, and since the peaks are close together this indicates that this complex is close to the crossover point between the ${}^4A_{2g}$ and ${}^4T_{1g}$ states on the energy diagram. This means that the assignments are only tentative, but the following assignments are commonly accepted:

$\nu_2({}^4T_{1g} \xrightarrow{(F)} {}^4A_{2g})$ 16000 cm^{-1} ✓

and $\nu_3({}^4T_{1g} \xrightarrow{(F)} {}^4T_{1g}(P))$ 19400 cm^{-1} ✓

The extra band is attributed either to spin orbit coupling effects or to transitions to doublet states.

Q Tetrahedral complexes of Co^{2+} such as $[CoCl_4]^{2-}$ are intensely blue in colour with an intensity ε of about 600 l mol^{-1} cm^{-1} compared with the pale pink colour of octahedral complexes with an intensity ε of only about 6 l mol^{-1} cm^{-1}, Co^{2+} has a d^7 electronic configuration, and in $[CoCl_4]^{2-}$ the electrons are arranged $(e_g)^4(t_{2g})^3$. This is similar to the Cr^{3+} (d^{3+}) octahedral case since only two electrons can be promoted. There are three possible transitions: ${}^4A_2(F) \rightarrow {}^4T_2(F)$, ${}^4A_2(F) \rightarrow {}^4T_1(F)$ and ${}^4A_2(F) \rightarrow {}^4T_{1g}(P)$. Only one band appears in the visible region at 15000 cm^{-1}. This band is assigned ν₃. There are two bands in the infrared region at 5800 cm^{-1} assigned ν₂ and the lowest energy transition (assigned ν₁) is expected at 3300 cm^{-1}.

$Cr^{3+} \Rightarrow d^5$

$Cr^{3+} =$

$Cr^{3+} =$

$Cr^{3+} = d^3$

${}^4A_2 \rightarrow {}^4T_1(P)$	ν_3	15000 cm^{-1} in the visible region ✓
${}^4A_2 \rightarrow {}^4T_1(F)$	ν_2	5800 cm^{-1} in the infrared region
${}^4A_2 \rightarrow {}^4T_2$	ν_1	(3300 cm^{-1} in the infrared region)

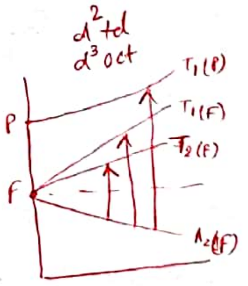

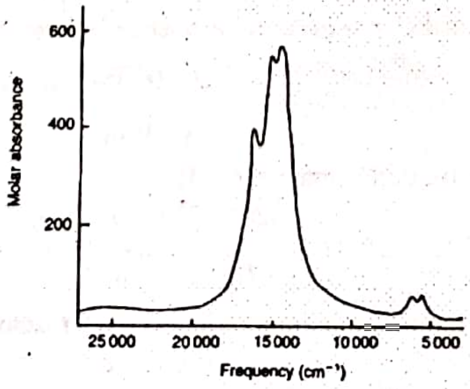

Fig. Electronic spectrum of $[CoCl_4]^{2-}$

Spectra of d^5 ions

The d^5 configuration occurs with Mn(II) and Fe(III). In high-spin octahedral complexes formed with weak ligands, for example $[Mn^{II}F_6]^{4-}$, $[Mn^{II}(H_2O)_6]^{2+}$ and $[Fe^{III}F_6]^{3-}$, there are five unpaired electrons with parallel spins. Any electronic transition within the d level must involved a reversal of spins, and in common with all other 'spin forbidden' transitions any absorption abnds will be extremely weak. This accounts for the very pale pink colour of most Mn(II) salts, and the pale violet colour of iron(III) alum. The ground state term is ^6S $^6S = {}^6A_{1g}$ None of the 11 excited states can be attained without reversing the spin of an electron, and hence the probablity of such transitions is extremely low. Of the 11 excited states, the four quartets ^4G, ^4F, ^4D and ^4P involved the reversal of only one spin. The other seven states are doublets, are double spin forbidden, and are unlikely to be observed. In an octahedral field these four split into ten states, and hence up to ten extremeley weak absorption bands may be observed. The spectrum of $[Mn(H_2O)_6]^{2+}$ is shown in figure. Several feature of this spectrum are unusual.

10 bands

1. The bands are extremely weak. The molar absorption coefficient ε is about 0.02 – 0.03 ℓ mol^{-1} cm^{-1}. Compared with 5-10 l mol^{-1} cm^{-1} for spin allowed transitions.
2. Some of the bands are sharp and other are broad. Spin allowed bands are invariably broad.

d^5 → +2 +1 0 −1 −2 [↑|↑|↑|↑|↑]

L = 0 = S shell = S state

$\frac{1}{2} \times 5 = \frac{5}{2}$

$2S+1 = 2 \times \frac{5}{2} + 1 = 6$

^6S g.s.

↓

^4G, ^4F, ^4D, ^4P

d^5 octahedral
$= d^5$ tetrahedral
$= d^{10}$ octahedral

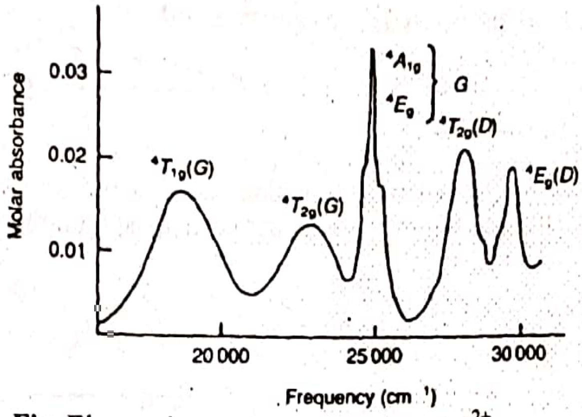

Fig. Electronic spectrum of $[Mn(H_2O)_6]^{2+}$

(11) The Widths of Observed Bands

Consider again the visible spectrum for $[Ti(H_2O)_6]^{3+}$. The single absorption abnd is quite broad, extending over several thousand wave numbers. The breadth of the absorption can be attributed mainly to the fact taht the complex is not a rigid, static structure. Rather, the metal-ligand bonds are constantly vibrating, with the result that an absorption peak is integrated over a collection of molecules with slightly different molecular structures and Δ_0 values. Such ligand motions will be exaggerated through molecular collisions in solution. In the solid state, however, it is sometimes possible to resolve spectral bands into their vibrational components. Sharp peaks also occur in solution spectra when the transitions involve ground and excited states that are either insensitive to changes in Δ_0 or are affected identically by the changes.

Two additional factors that can contribute to line breadth and shape are spin-orbit coupling, which is particularly prevalent in complexes of the heavier transition metals, and departures from cubic symmetry, such as through the Jahn-Teller effect.

(12) Jahn-Teller Distortions and Spectra

Up to this point, we have not discussed the spectra of d^1 and d^9 complexes. By virtue of the simple d-electron configurations for these cases, we might expect each to exhibit one absorption band corresponding to excitation of an electron from the t_{2g} to the e_g levels:

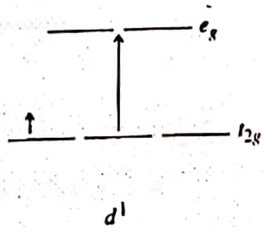

d^1

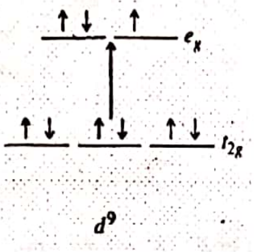

d^9

However this view must be at least a modest oversimpification, because examination of the spectra of

$[Ti(H_2O)_6]^{3+}(d^1)$ and $[Cu(H_2O)_6]^{2+}(d^9)$ shows these coordination compounds to exhibit two closely overlapping absorption bands rather than a single band.

To account for the apparent splitting of bands in these example, it is necessary to recall that, some configurations can cause complexes to be distorted. In 1937, Jahn and Teller showed taht nonlinear molecules having a degenerate electronic state should distort to lower the symmetry of the molecule and to reduce the degeneracy; this is commonly called the Jahn-Teller theorem. For example, a d^9 metal in an octahedral complex has the electron configuration $t_{2g}{}^6e_g{}^3$; according to the Jahn-Teller theorem, such a complex should distort. If the distortion takes the form of an elongation along the z axis (the most common distortion observed experimentally), the t_{2g} and e_g orbitals are affected as shown in following figure. Distortion from O_h to O_{4h} symmetry results in stabilization of the molecule: the e_g orbital is split into a lower a_{1g} level and a higher b_{1g} level.

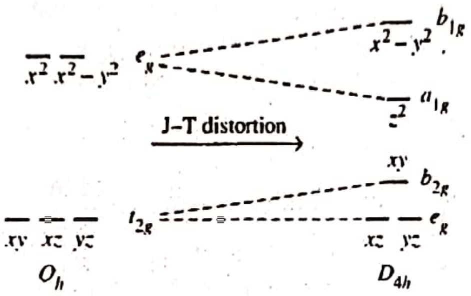

When degenerate orbitals are symmetrically occupied. Jahn-Teller distortions are likely. For example, the first two configurations below should give distortions, but the third and fourth should not:

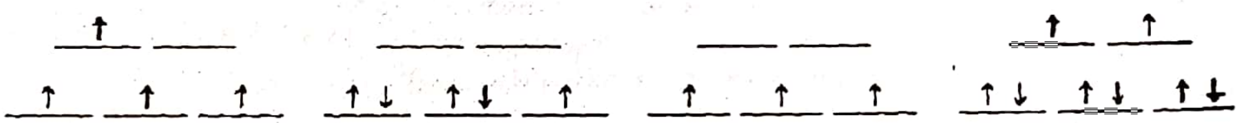

In practice, the only electron configuration for O_h symmetry that give rise to measurable Jahn-Telller distortions are those that have asymmetrically occupied e_g orbitals, such as the high spin d^4 configuration. The Jahn-Teller theorem does not predict what the distortion will be; by far, the most common distortion observed is elongation along the z axis. Although the Jahn-Teller theorem predicts that configurations having asymmetrically occupied t_{2g} orbitals, such as the low-spin d^5 configuration, should also be distorted, such distortions are two small to be measured in most cases.

The Jahn-Teller effect on spectra can easily be seen from the example of $[Cu(H_2O)_6]^{2+}$, a d^9 complex. From above figure, which shows the effect on d orbitals of distortion from O_h to D_{4h} geometry, we can see the additional splitting of orbitals accompanying the reduction of symmetry.

Symmetry Labels for Configurations

Electron configurations have symmetry labels that match their degeneracies, as follows:

		Examples
T	designates a triply degenerate asymmetrically occupied state.	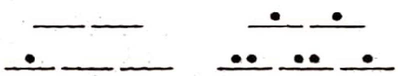
E	designates a doubly degenerate asymmetrically occupied state.	
A or *B*	designate a nondegenerate state. Each set of levels in an *A* or *B* state is symmetrically occupied.	

When a ^2D term for d^9 is split by an octahedral igand field, two configrations results:

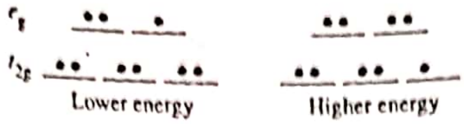

The lower energy configuration is doubly degenrate in the e_g orbitals (occupation of the e_g orbitals could be $\underline{\cdot\cdot}$ $\underline{\cdot}$ or $\underline{\cdot}$ $\underline{\cdot\cdot}$) and has the designation ^2E_g; the higher energy configuration is triply degenrate in the t_{2g} levels (three arrangements are possible in these levesl : $\underline{\cdot\cdot}$ $\underline{\cdot}$ $\underline{\cdot\cdot}$, $\underline{\cdot\cdot}$ $\underline{\cdot\cdot}$ $\underline{\cdot}$ or $\underline{\cdot}$ $\underline{\cdot\cdot}$ $\underline{\cdot\cdot}$) and has the designation $^2T_{2g}$. Thus, the lower energy configuration is the ^2E_g, and the higher energy configuration $^2T_{2g}$, as in the following figure. This is the opposite of the order of energies of the orbitals (t_{2g} lower than e_g), shown in figure.

Similarly, for distortion of D_{4h}, the order of labels of the orbitals in figure is the reverse of the order of labels of the energy configurations in figure.

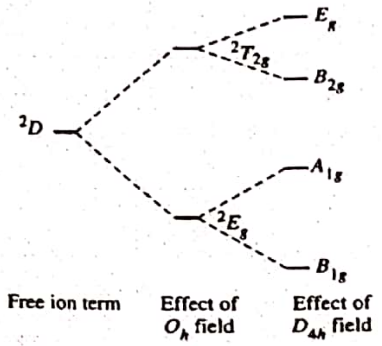

In summary, the ^2D free ion term is split into ^2E_g and $^2T_{2g}$ by a field of O_h symmetry, and further split on distortion to D_{4h} symmetry. The labels of the states resulting from the free-ion term are in reverse order to the labels on the orbitals; for example, the b_{1g} atomic orbital is of highest energy, whereas the B_{1g} state originting from the ^2D free-ion term is of lowest energy.

For a d^9 configuration, the ground state in octahedral symmetry is a ^2E_g term and excited state is a $^2T_{2g}$ term. On distortion to D_{4h} geometry, these terms split, as shown in figure. In an octahedral d^9 complex, we would expect excitation from the ^2E_g state to the $^2T_{2g}$ state and a single absorption band. Distortion of the complex to D_{4h} geometry splits the $^2T_{2g}$ levels into two levesl, the E_g and the B_{2g}. Excition can now occur from the ground state (now the B_{1g} state) to the A_{1g}, the E_g, or the B_{2g} (the splitting is exaggerated in figure). The $B_{1g} \rightarrow A_{1g}$ transition is too low in energy to be observed in the visible spectrum. If the distortion is strong enough, therefore, two separte absorption bands may be observed in the visible region, to the E_g or the B_{2g}. levels (or a broadened or narrowly split peak is found, as in $[Cu(H_2O)_6]^{2+}$).

For a d^1 complex, a single absorption band, corresponding to excitation of a t_{2g} electron to an e_g orbital, might be expected:

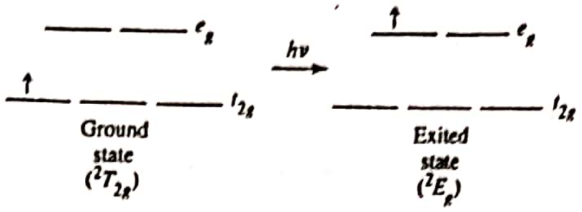

However, the spectrum of $[Ti(H_2O)_6]^{3+}$, an example of a d^1complex, shows two apparently overlapping bands rather than a single band. How is this possible?

One explanation commonly used is that the excited state can undergo Jahn-Teller distortion, as in figure. As in the examples considered previously, asymmetric occupation of the e_g orbitals can split these orbitals into two of slightly different energy (of A_{1g} and B_{1g} symmetry). Excitation can now occur from the t_{2g} level to either of these orbitals. Therefore, as in the case of the d^9 configuration, there are now two excited states of slightly different energy. The consequence may be a broadening of a spectrum into a two-humped peak, as in $[Ti(H_2O)_6]^{2+}$, or in some cases into two more clearly defined separte peaks.

UNIT-VII Charge Transfer Spectra

An electronic transition between orbitals that are centred on different atoms is called charge transfer transition and absorption band is usually very strong. These transitions involve electron transfer from one part of a complex to another. More specifically, an electron moves from an orbital that is mainly ligand in charcter to one that is mainly metal in character (ligand-to-metal charger transfer, LMCT) or vice versa (metal-to-ligand charger transfer, MLCT). Unlike *d-d* transitions, those involving charge transfer are fully allowed and hence give rise to much more intense absorptions. When these absorptions fall within the visible region, they often produce rich colors. In these electronic transitions, the electronic transitions are laporte and spin allowed, i.e.,

$$\Delta l = \pm 1 \text{ and } \Delta S = 0$$

A charge transfer transition may be regarded as an internal redox process.

Types of Charge Transfer Spectra

(1) Ligand to Metal Charge Transfer (LMCT)
(2) Metal to Ligand Charge Transfer (MLCT)
(3) Intermetal Charge Transfer or Metal to Metal Charge Transfer
(4) Interligand Charge Transfer

M → ① High Ionization Energ
↓
Empty orbital with low energ

M → hig oxidation state

(1) Ligand to Metal Charge Transfer (LMCT)

If the migration of electron is from ligand to the metal, then the charge transer is called ligand to metal charge transfer (LMCT). To make the electron transfer from ligand to metal more favorable, we require a metal with a relatively high ionization energy so that it would have empty orbitals at fairly low energies. The metals would be transition or posttransitions metals, or metals of main group with low ionisation energy, especially in higher oxidation states. An ideal ligand would be a nonmetal with a relatively low electron affinity, which would mean that it would have filled orbitals of fairly high energy and would be readily oxidizable. Chalcogenides or heavier halides or oxygen sulphur would be examples of good choices. The net result of such a metal-ligand combination would be that the orbitals involved in an LMCT process would be close enough in energy that the transition could be induced by a photon in the visible or near-ultrviolet region.

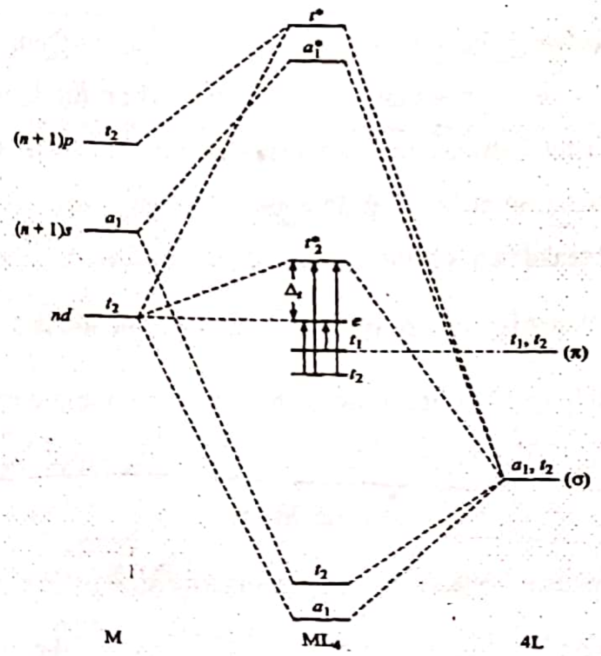

Figure (1)

The permanganate ion, MnO_4^-, Manganese is in a formal oxidation state of + 7 and combined with four oxide ions. The molecular orbital diagram for tetrahedral complexes in figure (1) allows us to identify possible LMCT transitions. In any tetrahedral complex, the four lowest energy σ-bonding orbitals will be filled and will be primarily ligand in character. Next there are two sets of σ-nonbonding MO's, one ligand-centered and one metal-centered. The permanganate, these orbitals would correspond to filled oxygen π_p orbitals and empty manganese 3*d* orbitals, respectively. All of the higher energy antibonding molecular orbitals would be unoccupied for a manganese (VII) complex. Hence there are four possible ligand-to-metal transitions:

$$L(t_1) \longrightarrow M(e)$$

$$L(t_1) \longrightarrow M(t_2^*)$$

$$L(t_2) \longrightarrow M(e)$$

$$L(t_2) \longrightarrow M(t_2^*)$$

For MnO_4^- all four of these transitions have been observed: 17,700 cm^{-1} ($t_1 \rightarrow e$); 29500 cm^{-1} ($t_1 \rightarrow t_2^*$); 30,300 cm^{-1} ($t_2 \rightarrow e$); and 44,400 cm^{-1} ($t_2 \rightarrow t_2^*$). Only the absorption at 17,700 cm^{-1} falls within the visible range (14,000 – 28,000 cm^{-1}), and it is responsible for the familiar deep purple colour of MnO_4^-.

In a similar way, the charge transfer spectrum of organge CrO_4^{2-} ion can be analyzed, the LMCT process being facilitated by the high oxidation state of chromium (VI). Many iodide salts also are colored becaused of charge transfer transitions of this type. Examples are HgI_2 (red), BiI_3 (orange-red) and PbI_2 (yellow). The metal ions in these substances certainly are not outstanding oxidizing agents, but the transitions occur because the iodide ion is easily oxidized.

Pigments in which colour is produced by LMCT are given below:

Pigment	**Primary orbitals involved**
Cadmium yellow (CdS)	Ligand $\pi_p \longrightarrow$ metal 5*s*
Vermilion (HgS)	Ligand $\pi_p \longrightarrow$ metal 6*s*
Naples yellow [$Pb_3(SbO_4)_2$]	Ligand $\pi_p \longrightarrow$ metal 5*s* or 5*p*
Massicot (PbO)	Ligand $\pi_p \longrightarrow$ metal 6*s*
Chrome yellow ($PbCrO_4$)	Ligand $\pi_p \longrightarrow$ metal 3*d*
Red and yellow ochres (iron oxides)	Ligand $\pi_p \longrightarrow$ metal 3*d*

reduc 2(2⁻ [illegible] oxidizing [illegible]

If the energy difference between the lowest unoccupied molecular orbital (LUMO) centered on the metal ion and the highest occupied molecular orbital (HOMO) centered on the ligand is very small (less than 10,000 cm^{-1}), total electron transfer between the two maay occur. This will be the case if the metal ion is a sufficiently good oxidizing agent and the ligand a good enough reducing agent to cause a spontaneous redox process. The result is breakdown of the complex. Examples of complexes in which this occurs are $[Co(H_2O)_6]^{3+}$ and FeI_3: Water is oxidized by Co^{3+} and the iodide ion is oxidized by Fe^{3+}.

Figure (2) shows the visible and UV spectrum of the less symmetric complex $[CrCl(NH_3)_5]^{2+}$. From this spectrum we can recognize the two ligand-field, *d-d*, bands in the visible region. The replacement of one NH_3 ligand by a weaker field Cl^- ligand moves the lowest energy *d-d* bands to lower energy than those of $[Cr(NH_3)_6]^{3+}$. Also, a shoulder appears on the high-energy side of one of the *d-d* bands as a result of the reduction in symmetry from O_h to C_{4v}. Another new feature in the spectrum is the strong absorption maximum in the ultraviolet, near 42,000 cm^{-1}. This band is at lower energy than the corresponding band in the spectrum of $[Cr(NH_3)_6]^{3+}$ and has been assigned as an LMCT transition from the Cl^- ligand to the metal.

The LMCT character of similar bands in $[CoX(NH_3)_6]^{2+}$ is confirmed by the decrease in wavenumber in steps of about 8000 cm^{-1} as X is varied from Cl to Br to I. In this LMCT transition a lone-pair electron of the halide ligand is promoted into a predominantly metal orbital.

Charge-transfer transitions are identified by their high intensity and the sensitivity of their energies to

solven polarity.

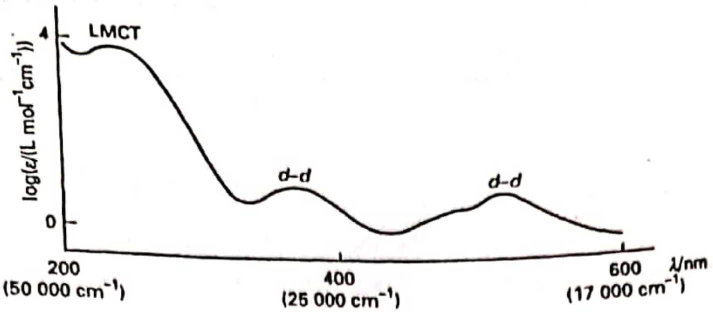

Figure (2)

CT transitions are generally intense compared with ligand-field transitions. Charge-transfer bands in the visible region of the spectrum (and hence contributing to the intense colors of complexes) may occur if the ligands have lone pairs of relatively high energy (as in sulfur and selenium) or if the metal has low-lying empty orbitals. The color of the artists pigment 'cadmimum yellow', CdS, for instance, is due to the transition Cd^{2+} (5s) ← S^{2-} (π). Similarly, HgS is red as result of the transition Hg^{2+} (6s) ← S^{2-} (π) and others are iron oxides that are colored red and yellow by the transition Fe (3d) ← O^{2-} (π).

The tetraoxoanions of metals with high oxidation numbers (such as MnO_4^-) provide what are probably the most familiar examples of LMCT bands. In them, an O lone-pair electron is promoted into a low-lying empty d metal orbital. High metal oxidation states correspond to a low d-orbital population (many are d^0), so the acceptor level is available and low in energy. The trend in LMCT energies is:

Oxidation Number	
+ 7	$MnO_4^- < TcO_4^- < ReO_4^-$
+ 6	$CrO_4^{2-} < MoO_4^{2-} < WO_4^{2-}$
+ 5	$VO_4^{3-} < NbO_4^{3-} < TaO_4^{3-}$

→ 3d Energy Mn < For 4d of TC < 5d Re
good CT transfer
S. a copy

The energies of the transitions correlate with the order of the electrochemical series, with the lowest energy transitions taking place to the most easily reduced metal ions. This correlation is consistent with the transition being the transfer of an electron from the ligands to the metal, corresponding, in effect, to the reduction of the metal ion by the ligands.

Polymeric and monomeric oxoanions follows the same trends, with the oxidation number of the metal the determining factor.

The variation in the position of LMCT bands can be expressed in terms of the optical electronegativities of the metal, χ_{metal} and the ligands, χ_{ligand}. The wavenumber of the transition is then writeen as the difference between the two electronegativities:

$$\tilde{\nu} = |\chi_{ligand} - \chi_{metal}|\tilde{\nu}_o$$

Optical electronegativities have values comparable to pauling electronegativities if we take the constant $\tilde{\nu}_0$ to be 3.0×10^4 cm^{-1}. If the LMCT transition terminates in an e_g orbital, Δ_0 must be added to the energy predicted by this equation. Electron pairing energies must also be taken into account if the transition results in the population of an orbital that already contains an electron. The values for metals are different in complexes of different symmetry, and the ligand values are different if the transition originates from a π orbital rather than a σ orbital.

Ligand-to-metal transitions are observed when the metal is in a high oxidation state and ligands contain lone-pair electrons, the variation in the position of LMCT bonds can be parametrized in terms of optical electronegativities.

The spectra of $RuCl_6^{2-}$ and $IrBr_6^{2-}$ (d^4 and d^5 complexes, respectively) show two sets of bands that have been assigned to transitions from the weakly bonding π orbitals on the ligands to the antibonding t_{2g}^* and e_g^* orbitals of the metal atom. In $IrBr_6^{2-}$ (a d^6 complex), the t_{2g}^* orbitals are filled, and only the transition to the e_g^* orbitals can be observed.

In the halogenopentaammine complexes of the type $Co(NH_3)_5X^{2+}$, strong charge-transfer bands are observed in the ultraviolet region. These bands appear at progressively lower frequencies on going from the chloro to the bromo to the iodo complex, as one might expect from the trend in reduction potentials for these halogens. Indeed, in $Co(NH_3)_5I^{2+}$, the charge-transfer bands largely obscure the weaker *d-d* transitions.

(2) Metal to Ligand Charge Transfer (MLCT)

Ligand → Empty π antibonding

If the migration of electron is from metal to ligand, then charge transfer is called metal to ligand charge transfer (MLCT). Charge transfer processes in the opposite direction, from metal to ligand, are favored in complexes that have occupied metal-centered orbitals and vacant low lying ligand-centered orbitals. Prime examples are complexes in which the ligands have empty π antibonding orbitals. Ligands falling into this category include CN^-, SCN^- carbon monoxide, pyridine, bipyridine, pyrazine, *o*-phenanthroline, dithiolene ($S_2C_2R_2$), dithiocarbamate (S_2CNR_2) shows possible MLCT transitions for an octahedral complex in which both the t_{2g} and e_g orbitals are occupied.

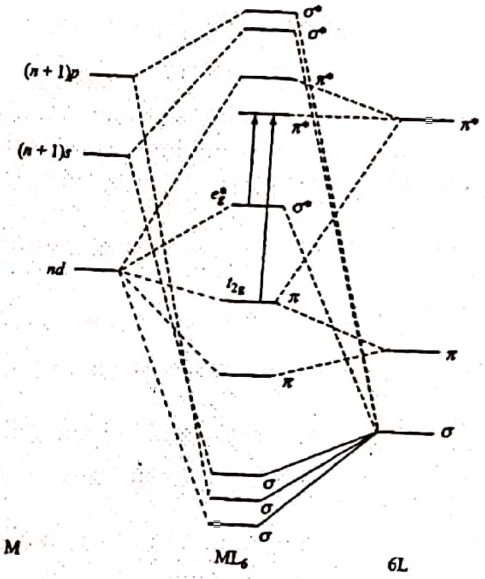

Figure (3)

An example of an MLCT transition is the one responsible for the red color of tris(bipyridyl)iron(II), the complex used for the colorimetric analysis of Fe(II). In this case, an electron makes a transition for a *d* orbital of the central metal into a π^* orbital of the ligand.

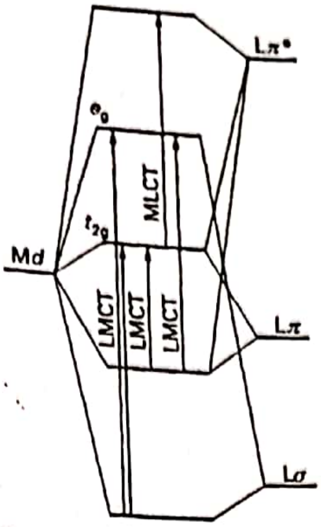

Figure (4)

Diamines, which have two N donor atoms: two important examples are 2, 2'-bipyridine and 1, 10-phenanthroline. Complexes of diimines with strong MLCT bands include tris(diimine) species such as tris (2, 2'bipyridyl)ruthenium(II), which is orange on account of its MLCT band. A diimine ligand may also be easily substituted into a complex with other ligands that favor a low oxidation state. Two examples are [W(CO)$_4$(phen)] and [Fe(CO)$_3$(bipy)]. However, the occurrence of MLCT transitions is by no means limited to diimine ligands. Another important ligand type that shows typical MLCT transitions is dithiolene, $S_2C_2R_2$. Resonance Raman spectroscopy is a powerful technique for the study of MLCT transitions, particularly of diimine complexes.

Charge transfer transitions from metal to ligand are most commonly observed in complexes with ligands that have low lying π* orbitals specially aromatic ligands.

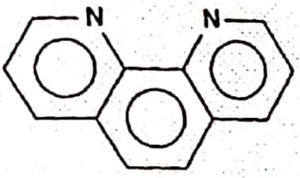
5 1,10–Phenthroline (phen)

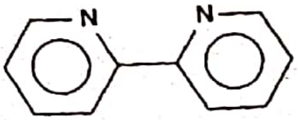
4 2,2′–Bipyridine (bipy)

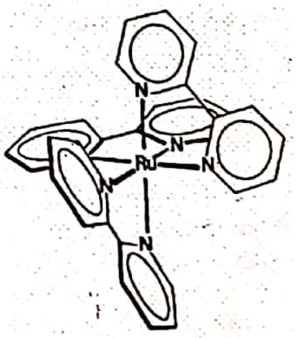
6 [Ru(bipy)$_3$]$^{2+}$

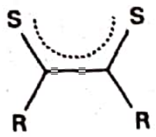
7 Dithiolene

The visible absorption spectra of iron(II) complexes with ligands containing the α-diimine unit

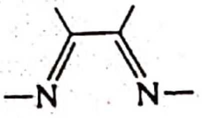

have intense charge-transfer bands associated with the transfer of charge from metal t_{2g} orbitals to the antibonding orbitals of the α-diimine group. In the case of the 1, 10-phenanthroline complex $Fe(phen)_3^{2+}$, the transition occurs at 19,600 cm^{-1}. A series of 6-coordinate iron(II) complexes containing the tetraimine macrocyclic ligand (TIM) shown below, have been prepared with various monodentate liands occupying the two axial sites. The band maxima of these complexes, corresponding to metal-to-TIM charge transfer, are given below. It can be seen that the transition energy is a function of the π-acceptor ability of the axial ligands. As the π-acceptor ability increases, the energy of the d_{xz} and d_{yz} orbitals decreases relative to that of the π (TIM) orbital, causing the $t_{2g} \to \pi$ (TIM) charge-transfer band to move to higher energies.

Complex	Band maximum cm^{-1}
$Fe(TIM)CH_3CN(CO)^{2+}$	23,200
$Fe(TIM)(P(OEt)_3)_2^{2+}$	19,500
$Fe(TIM)(CH_3CN)_2^{2+}$	18,200
$Fe(TIM)(imidazole)_2^{2+}$	15,200
$Fe(TIM)(NH_3)_2^{2+}$	14,300

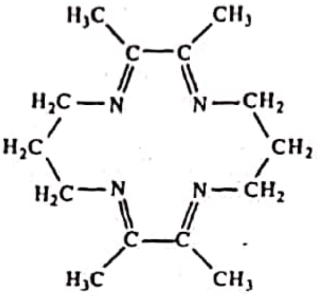

TIM

Spectra of Compounds with Metal-Metal Bonds

Compounds which contain metal-metal bonds are intensely colored. For example $Mn_2(CO)_{10}$ is bright yellow, $Re_2Cl_8^{2-}$ is deep blue, $Co_2(CO)_8$ is purple-black, $Mo_2Cl_8^{4-}$ is cherry red, and $Fe_2(CO)_9$ is gold; the observed transitions for these compounds are of the types $\sigma \to \sigma^*$, $\pi \to \pi^*$ and $\delta \to \delta^*$ and are fully allowed. In the case of $Mn_2(CO)_{10}$, the $\sigma \to \sigma^*$ band peaks at 29,400 cm^{-1}. One expects that this excitation should be accompanied by weakening or dissociation of the Mn-Mn bond. Indeed, ultraviolet irradiation of $Mn_2(CO)_{10}$ in carbon tetrachloride solution leads to the intermediate formation of $Mn(CO)_5$ radicals, which abstract chlorine atoms from the solvent to form the chlorine-substituted mononuclear complex:

$$Mn_2(CO)_{10} \xrightarrow[CCl_4]{h\nu} 2Mn(CO)_5Cl$$

$\sigma \to \sigma^*$
$\pi \to \pi^*$
$\delta - \delta^*$
$2Mn_2(CO)_{10} \xrightarrow[CCl_4]{h\nu} 2Mn(CO)_5^{\cdot} \downarrow Cl$
$2Mn(CO)_5Cl$

Photochemical cleavage of metal-metal bonds is fairly common in metal cluster compounds. However, it appears that excitation to the relatively weakly antibonding π* and δ* states is ineffective for such cleavage.

(3) Intermetal Charge Transfer

Potassium ferrocyanide is used to test for iron in solution. Fe^{2+} ions give a white precipitate of $K_2Fe^{II}[Fe^{II}(CN)_6]$, but Fe^{3+} ions give deep blue $KFe^{III}[Fe^{II}(CN)_6]$ known as Prussian blue. A deep blue colour is also produced by Fe^{2+} with $K_3[Fe^{III}(CN)_6]$, and this is known as Turnbull's blue $KFe^{II}[Fe^{III}(CN)_6]$. Both have been used as pigments in ink and paint. Recent X-ray work, infrared and Mossbauer spectroscopy have shown that Turnbull's blue is identical to Prussian blue. The intense colour arises from electron transfer between Fe(+II) and Fe(+III).

$[K_4Fe(CN)_6]$
$K_2Fe^{II}[Fe^{II}(CN)_6]$
$KFe^{III}[Fe^{II}(CN)_6]$
blue
$\rightleftharpoons$
$KFe^{II}[Fe^{III}(CN)_6]$

(4) Interligand Charge Transfer

The ligand itself may have a chromophore and still another type of absorption band, an intraligand band, may be observed. These bands may sometimes be identified by comparing the spectra of complexes with the spectra of free ligands. However, coordination of ligand to a metal may significantly alter the energies of the ligands orbitals, and such comparisons may be difficult, especially if charge-transfer bands overlap the intraligand bands. Also, it should be noted that not all ligands exist in the free state; some ligands owe their existence to the ability of metal atoms to stabilize molecules that are otherwise highly unstable.

$Cu_2O \to$ charge tran

Some Other Examples of Charge Transfer Spectra

1. In the (+1) state of Cu most of the simple compounds and complexes are diamagnetic and colourless because the ions have a d^{10} configuration. There are a few coloured compounds. For example, Cu_2O is yellow or red, Cu_2CO_3 is yellow and CuI is brown. In these cases the colour arises from charge transfer bands and not from

d-d spectra.

2. There are several blue proteins which contain Cu. They act as electron transfer agents by means of a Cu^{2+}/Cu^{+} couple. Their colour is much more intense than would be expected for *d-d* spectra. The colour is thought to be caused by charge transfer between Cu and S. Examples include plastocyanin and azurin. Plastocyanin occurs in the chloroplasts of green plants.
3. Zn, Cd and Hg have a d^{10} electronic configuration and so cannot produce *d-d* spectra. Thus many of their compounds are white. However, some compounds of Hg (+II) and a smaller number of Cd (+II) are highly coloured due to charge transfer from the ligands to the metal.
4. HgI_2 exists in red and yellow forms. The colour is due to charge transfer.
5. The orange colour of SnI_4 is caused by the absorption of blue light, the reflected light thus containing a higher proportion of red and orange. The energy absorbed in this way caused the transfer of an electron from I to Sn. (This corresponds to the temporary reduction of Sn(IV) to Sn(III). Since transferring an electron to another atom is transferring a charge, such spectra are called charge transfer spectra. This occurs in SnI_4 and GeI_4 because the atoms have similar energy levels. This would be expected because they are close in the periodic table, and have similar sizes. Charge transfer spectra do not occur with the other halides.
6. Almost all manganese compounds are coloured. Mn^{2+} is pale pink, and MnO_2 is black, both becauseof *d-d* transitions. The (+ VII) oxidation state has a d^0 configuration and would be expected to be colourless. Whilst perrhenates ReO_4^- containing Re (+VII) are colourless, permanganates MnO_4^- containing Mn (+VII) are intensely coloured. The purple-black colour arises from charge transfer spectra.
7. The permanganate MnO_4^- ion has an intense purple colour. Mn (+VII) has a d^0 configuration, so the colour arises from charge transfer and not from *d-d* spectra.
8. $KMnO_4$ is a very dark purple-black solid. The MnO_4^- ion is deep purple coloured due to charge transfer spectra. In contrast solutions of TeO_4^- and ReO_4^- are colourless, as the charge transfer band occurs at higher energy in the UV region. However solutions of $HReO_4$ become yellow-green when they are concentrated, and $HTcO_4$ has been isolated a red solid. These colours arise because the tetrahedral ReO_4^- ion becomes less symmetrical when undissociated HO—ReO_3 is formed.
9. $Cr_2O_7^{2-}$ is an orange solid, CrO_4^{2-} is yellow solid, CrO_3 is a bright orange solid. The colour arises from charge transfer (not *d-d* spectra as Cr (+VI) has a d^0 configuration.
10. V_2O_5 is orange or red coloured due to charge transfer.

MnO_4^{2-} → Charge transfe

MnO_2 → dd tra

Cu_2O → Charge transfer

V_2O_5 → charge tr